# COUPLED EDGE PROFILE ACTIVE CONTOURS FOR RED BLOOD CELL FLOW ANALYSIS

*I. Ersoy*[1], *F. Bunyak*[1], *J.M. Higgins*[2,3], *K. Palaniappan*[1]

[1]University of Missouri Columbia
Department of Computer Science
Columbia, MO 65201

[2]Department of Systems Biology
Harvard Medical School, Boston, MA 02115
[3]MGH Center for Systems Biology, Boston, MA 02114

## ABSTRACT

Physiological properties of blood flow at the microvasculature scale can be measured by tracking the movement and density of red blood cells (RBCs). In this paper we propose a method for individual RBC segmentation to enable tracking and capturing dynamically varying bulk transport properties. RBCs have varying annular and disk like morphologies, and are often clustered into clumps that are difficult to segment using watershed-based methods. Edge profile active contours in combination with graph coloring based coupling (C-EPAC) are introduced as a robust approach to prevent merges between adjacent, clumped RBCs by modifying the active contour energy function to be sensitive to a specific edge profile and not just the magnitude as in the traditional methods. Explicit coupling is combined with graph coloring to efficiently compute the contour evolution using the fewest number of level sets to support high-throughput studies of RBC flow characterization under varying physiological conditions.

***Index Terms***— cell segmentation, level set active contours, red blood cells, cell tracking.

## 1. INTRODUCTION

Measuring the flow dynamics of red blood cells (RBCs) is important for quantitatively characterizing phenomena such as nutrient and gas transport, clumping and clotting, sickle cell behavior and vascular occlusions. The majority of blood flow analysis studies with few exceptions [1–3] focus primarily on mean flow properties which lack the single cell resolution needed to quantify accurate time varying flow parameters. The flow characteristics of blood plasma suspensions are largely determined by the dynamic behavior of the suspended particles [4], so studying the behavior of single red blood cells and their collective motion will provide a better quantitative understanding of the rheology of blood flow. In order to characterize the dynamic behavior of microvasculature flows, individual RBCs need to be detected, segmented and tracked. The segmentation and tracking of red blood cells introduce unique challenges. Red blood cells usually occupy more than one-third of the volume in blood. They interact with each other and with the environment due to effects of varying cell concentration, cell morphology, cell rheology, and confinement. These interactions result in dynamically changing collision and clustering effects, which along with variability of appearances (annular versus filled cells) make segmentation and subsequently tracking of individual cells challenging. While tracking few individual cells may be adequate to estimate mean flow properties, it is also important to accurately segment and track *clustered* cells in order to effectively quantify hydrodynamic interactions between cells that lead to velocity fluctuations and diffusive dynamics of individual cells. This paper presents a robust and efficient approach that combines a voting-based seed detection and a novel active contour cell segmentation method to accurately segment individual RBCs. Individual cell level and population level statistics can be computed by a multi-hypothesis testing multi-cell tracking module [5] following the segmentation. Exploiting the fact that the red blood cells are in circular or annular shape, we propose an approach that uses an improved iterative voting scheme similar to [6] to reliably generate initial markers for individual cells. Starting from these seeds/markers, the proposed coupled edge profile active contours (C-EPAC) expand to correct boundaries of RBCs. This novel method enables correct segmentation of both filled and annular cells by forcing the active contours to stop on specific edge profiles. Multiple cells are segmented simultaneously by using an explicit coupling scheme that efficiently prevents merging of cells in clusters.

## 2. METHODS

### 2.1. Individual cell seed detection

Segmentation of individual cells is an important and challenging necessity for biomedical image analysis studies. Analysis of cell morphology (shape, structure, color, texture), distribution in still images, and cell motility/behavior in image sequences heavily rely on identification of individual cells. Due to high density, collisions, and interactions, red blood cells tend to form tight clusters. Various approaches have been proposed for cluster decomposition and for individual center or seed point detection. An extensive overview of related work can be found in [7]. The proposed system detects individual RBC centers using a technique based on iterative voting approach described in [6]. The method applies a series of cone-shaped kernels (Figure 1a) to potential cell boundary points. These kernels generate votes along the radial directions whose accumulation results in a peak in the voting space located at the center of a circular object. The iterative approach refines the center of mass at each iteration until it converges to a focal response. Figure 1 shows the final voting landscape and the resulting centers for a sample RBC cluster. We further improve this technique by applying a pre-filtering approach that reduces fragmentation (i.e. reducing multiple centers for a single nucleus), by improving the radial directions by exploiting both image gradient information and region segmentation information for better localization, and by post-validation of the centers by distance statistics.

### 2.2. Segmentation with edge profile active contours

While region-based active contours have been succesfully used in many cell and nucleus segmentation applications [8], they require

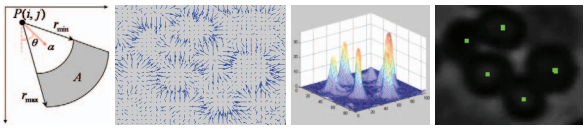


**Fig. 1**: Seed detection using iterative voting. a) iterative voting kernel, b) radial directions, c) vote surface after 2nd iteration, d) detected centers (seeds) overlayed on the original cell cluster image.

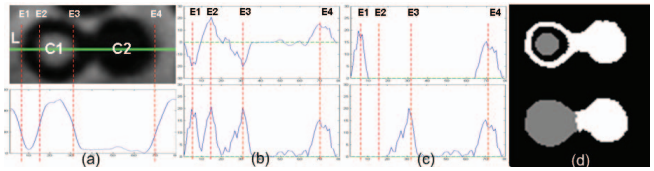


**Fig. 2**: Comparison of coupled-regular geodesic active contours( C-GAC) vs. proposed coupled- edge profile active contours (C-EPAC). a) An RBC cluster consisting of an annular and a filled cell with seed points *C1* and *C2* and the intensity profile along the marked green line *L*, b) Gradient and gradient magnitude profiles along *L*, c) Desired stopping edges for *C1* (top) and *C2* (bottom), d) Segmentation results C-GAC (top) and proposed C-EPAC (bottom).

homogeneous intensity inside the cell boundaries as well as in the background, hence they are not applicable in some cell imaging modalities. Figure 3a shows typical red blood cells, where a straightforward implementation of [8] would converge to the white regions inside the annular red blood cells as opposed to the correct boundaries. Extensions to multi-phase would also lead to similar segmentation. For these types of images where intensity inside the cell boundaries is heterogeneous, edge-based approaches are more suitable. The classical geodesic active contour approach [9] is designed to stop at edges regardless of the region characteristics. In level set based active contour methods, a curve $\mathcal{C}$ is represented implicitly via a Lipschitz function $\phi$ by $\mathcal{C} = \{(x, y)|\phi(x, y) = 0\}$, and the evolution of the curve is given by the zero-level curve of the function $\phi(t, x, y)$ [8]. In regular geodesic active contours [9] the level set function $\phi$ is evolved using the speed function,

$$\frac{\partial \phi}{\partial t} = g(\nabla \mathbf{I})(F_c + \mathcal{K}(\phi))|\nabla \phi| + \nabla \phi \cdot \nabla g(\nabla \mathbf{I}) \tag{1}$$

where $F_c$ is a constant, $\mathcal{K}$ is the curvature term (Eq.2) and $g(\nabla \mathbf{I})$ is the edge stopping function, a decreasing function of the image gradient which can be defined as in Eq.3.

$$\mathcal{K} = div\left(\frac{\nabla \phi}{|\nabla \phi|}\right) = \frac{\phi_{xx}\phi_y^2 - 2\phi_x\phi_y\phi_{xy} + \phi_{yy}\phi_x^2}{(\phi_x^2 + \phi_y^2)^{\frac{3}{2}}} \tag{2}$$

$$g(\nabla \mathbf{I}) = exp(-|\nabla G_\sigma(x, y) * \mathbf{I}(x, y)|) \tag{3}$$

The constant balloon force $F_c$ pushes the curve inwards or outwards depending on its sign. The regularization term $\mathcal{K}$ ensures boundary smoothness and $g(\mathbf{I})$ is used to stop the curve evolution at cell boundaries. This approach usually suffers from early stopping on irrelevant edges if not initialized properly. Initial contours are usually obtained by a detection step using spatial or spatio-temporal properties (e.g. [10, 11]), and the active contour shrinks from outside towards the cell boundary. For red blood cell segmentation, we follow a different approach where the seeds (initial markers) found by iterative voting serve as initial detections and the contours expand from the seeds to the cell boundaries. To obtain an accurate segmentation, we propose an expanding level set active contour that stops the evolving contour on the correct cell boundary based on the perpendicular edge profile. Both filled dark cells and annular cells have the same dark-to-bright profile on their outer boundaries as showin in Fig. 2 (edges *E1* and *E4*). Initializing with a seed at the center of the cell (Fig. 2 *C1* and *C2* ), the regular geodesic active contour would stop at the inner boundary (bright-to-dark transition) of the annular cell, resulting in an inaccurate segmentation (Fig. 2d top). The proposed active contour (C-EPAC) is guided by the desired edge profile which effectively lets the curve evolve through inner boundary of the annular cell and stop at the correct outer boundary as in Fig. 2c top (edges *E1,E4* for seed *C1*) and Fig. 2c bottom (edges *E3,E4* for seed *C2*). The stopping function of the proposed method is obtained as follows. Edge profile is obtained as the intensity derivative in the direction of evolving contour/surface normal $\vec{N}$:

$$\mathbf{I}_{\vec{N}} = \vec{N} \cdot \nabla \mathbf{I}\ ,\ \vec{N} = -\frac{\nabla \phi}{|\nabla \phi|} \tag{4}$$

Dark-to-bright transitions produce positive response in $\mathbf{I}_{\vec{N}}$ while expanding the contour from inside to outside. This is the desired transition to stop the contour, hence we define the edge profile-guided stopping function $g_d$ as:

$$g_d(\nabla \mathbf{I}) = 1 - \mathrm{H}(-\frac{\nabla \phi}{|\nabla \phi|} \cdot \nabla \mathbf{I})\ ,\ \mathrm{H}(x) = \begin{cases} 1 & \text{if } x > 0 \\ 0 & \text{elsewhere} \end{cases} \tag{5}$$

This sets $g_d$ to 1 at regions where there is a bright-to-dark transition (inner contour of annular cell) perpendicular to evolving level set, and to zero where there is a dark-to-bright transition (outer contour of annular cell). Thus it lets the active contour evolve through the annular cells without getting stuck at the inner boundaries. Eq.6 shows the speed function of the proposed curve evolution. Figure 2d shows a portion of a frame with annular and filled cells, where the regular geodesic active contour gets stuck at the inner contours of annular cells but the proposed method accurately evolves to the correct boundary.

$$\frac{\partial \phi}{\partial t} = g_d(\nabla \mathbf{I})(F_c + \mathcal{K}(\phi))|\nabla \phi| + \nabla \phi \cdot \nabla g_d(\nabla \mathbf{I}) \tag{6}$$

### 2.3. Explicit coupling for multiple cell segmentation and graph coloring

The level set active contour proposed in the previous section successfully segments a single cell with no neighboring cells. But for clustered RBCs that have no discernible boundaries between them, a single level set would produce a single lumped segmentation by merging all contours that expand from several seeds. In order to avoid merging, a N-level set approach has been proposed in [12] that assigns each cell a separate level set coupled with all other level sets. While this solves the merging problem, it is very computationally expensive and not scalable since it requires evolution of N level sets with $N^2/2$ couplings where N is around 100 cells per frame. In order to avoid the computational cost, we use constant number of level sets by utilizing the neighborhood relationships between cells. A similar graph approach is applied to Chan and Vese type level sets in [5]. We compute the Delaunay triangulation to obtain a graph of neighborhoods. By coloring this graph so that no two neighboring vertices have the same color, we separate neighboring cells into different level sets and reduce the number of level sets to constant

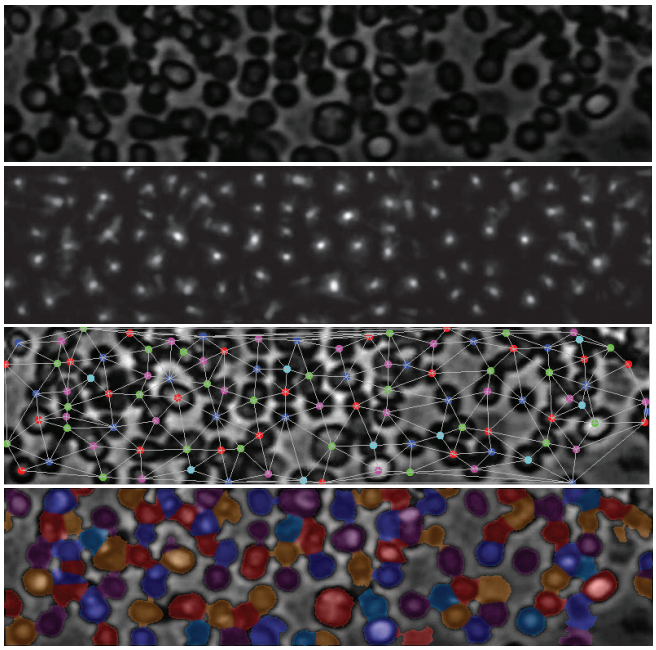

**Fig. 3**: Row 1: original image, row 2: iterative voting result, row 3: colored neighborhood graph, row 4: segmentation mask obtained using coupled edge profile active contours.

regardless of the number of cells. We employ a greedy coloring algorithm that produces five or six colors for the planar graph. Figure 3c shows a sample frame with Delaunay triangulation followed by graph coloring of cell markers. In order to explicitly control the topology evolution of these level sets so that no two cells merge, we propose a novel explicit coupling strategy (Eq.7) which stops any level set $\phi_i$ from intruding to the foreground region of any other level set $\phi_j$ by intersecting background masks of $\phi_j$ as the only permissible region for $\phi_i$ to expand:

$$\frac{\partial \phi_i}{\partial t} = [g_d(\nabla \mathbf{I})(F_c + \mathcal{K}(\phi_i))|\nabla \phi_i| + \nabla \phi_i \cdot \nabla g_d(\nabla \mathbf{I})] \prod_{j \neq i} (1 - H(\phi_j)) \tag{7}$$

## 3. EXPERIMENTAL RESULTS

RBC flow videos described in [4] are used for testing. These videos capture blood flow in microfluidic devices under controlled oxygen concentration. Blood flows through channels with crosssectional dimension of $250 \times 12$ mm and is driven by a constant pressure head. Videos are captured at a rate of 60 frames per second, with a resolution of about 6 pixels per micron. Figure 3 shows outputs of the major steps of the proposed RBC segmentation system on a sample frame. Figure 4 shows segmentation results obtained from the proposed coupled edge profile active contours (C-EPAC), marker-controlled watershed (MC-WAT) RBC segmentation as in [4], and coupled regular geodesic active contours (C-GAC). In all cases, centers found by iterative voting (Section 2.1) are used as initial markers, which is already an improvement compared to the morphological markers used in [4]. Both versions of the watershed approaches (Figure 4 (rows 1,2) suffer from different problems even though improved markers have been used, mainly due to the annular cells. In (Figure 4-row 3) improved voting-based seeds and the added coupling term greatly improve performance of regular GAC but inner edges of annular cells cause early stopping and consequently shape deformations. Proposed method C-EPAC (Figure 4-row 4) produces substantially better results in terms of recall of cells, separation of the clusters and accuracy of the obtained contours. This directly translates to increased number of reliable tracks and increased track lengths. Table 1 presents quantitative evaluation of methods MC-WAT, C-GAC, and proposed C-EPAC.Statistics are obtained by comparing automatic segmentation results to manual segmentations of 1008 cells. For a fair comparison, all the methods have been initialized with the same seeds obtained through iterative voting (Sec.2.1). Reported recall numbers are strictly computed using only 1-to-1 matches between ground truth cells and segmented cells, discarding any segmented cell that is fragmented or merged. When merged or fragmented cells are included, the recall percentages increase to 70%, 89%, and 91% for MC-WAT, C-GAC, and the proposed C-EPAC respectively. It is worth noting that these quantitative results evaluate the cell detection only and not the accuracy of cell shapes produced by the methods. As seen in Figure 4 the proposed method produces substantially more accurate cell shapes that increase the accuracy of the cell tracking module. Even though proposed method creates slightly more false positives (FP), they can be easily filtered in the subsequent tracking module by enforcing spatio-temporal persistence criteria whereas recovering from FN is not possible. The proposed method has the lowest FN and the highest recall that enables accurate tracking of maximum number of cells for accurate flow analysis.

| | FN | FP | Recall | Prec |
|---|---|---|---|---|
| MC-WAT | 20.5% | **0.2%** | 63.5% | **87.9%** |
| C-GAC | 3.6% | 1.1% | 67.3 % | 70.5% |
| C-EPAC | **1.7%** | 3.9% | **80.6%** | 81.5% |

**Table 1**: Segmentation performance compared to manual ground truth for MC-WAT: marker-controlled watershed on intensity, C-GAC: coupled geodesic active contours (using the proposed coupling method), and proposed C-EPAC: coupled edge profile active contours.

While significant tracking accuracy have been demonstrated for some applications and data sets in the past few years [13–15],success and reliability of cell/nuclei tracking remain to be highly dependent on image characteristics, cell population and environment characteristics, and accuracy of prior processing steps. For individual red blood cell tracking, we extended and adapted our cell tracking system in [5] with constraints specific to hydrodynamics of red blood cell flow. The proposed segmentation method ensures that clumped cells are individually tracked over time. Since the emphasis of this paper is not cell tracking, we briefly illustrate a sample tracking result for a flow sequence in Figure 5 using the proposed segmentation method. Trajectories for all the cells are shown as well as the longest tracks, and some simple displacement statistics, i.e. distribution of RBC displacements per frame. Other more elaborate and biologically more relevant statistics can be easily computed from the tracks. This result illustrates that the proposed method drastically improves the cell track lengths in comparison to [4].

## 4. CONCLUSION

We have introduced a robust RBC detection and segmentation approach that enables accurate tracking of individual cells and hence extraction of rich statistical information at individual cell level in-

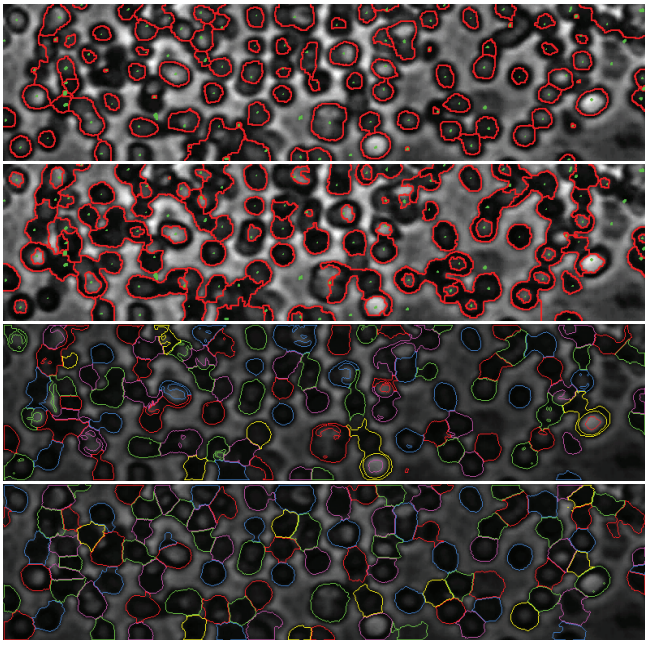

**Fig. 4**: Row 1: Marker-controlled watershed on intensity surface, row 2: Marker-controlled watershed on gradient of the intensity surface, row 3: Coupled geodesic active contours, row 4: Coupled edge profile active contours.

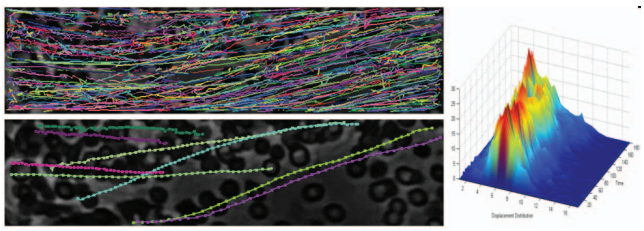

**Fig. 5**: Tracking results for a sample RBC flow sequence. Top: all trajectories, bottom: eight longest trajectories (track length $> 80$ frames, each tick corresponds to 2 frames), right: distribution of RBC displacements per frame over time.

cluding flow properties. It also enables accurate morphological analysis of cells for biologically relevant properties such as density and clumping behavior. As far as we are aware, C-EPAC is the only level set framework in which both annular and filled cells can be simultaneously segmented accurately. The extensions of Chan and Vese approach to multi-phase and piece-wise smooth level sets would fail to distinguish touching cells resulting in similar segmentations as shown in upper part of Fig.2d. This approach is grounded in image formation and can also be applied to general phase contrast imaging with high cell densities. Our explicit coupling strategy controls the topology evolution by preventing merging of neighboring cells in RBC clusters at a drastically reduced computational cost as opposed to traditional $O(N^2)$ coupling terms in N-level set approaches. Using this method and and our cell tracker, biologically relevant statistics can be accurately computed from the extracted long tracks for both normal and pathological flows which we will report in a future work.

## 5. REFERENCES


[1] C.C. Reyes-Aldasoro, S. Akerman, and G.M. Tozer, "Measuring the velocity of fluorescently labelled red blood cells with a keyhole tracking algorithm," *J. Microscopy*, vol. 229, no. 1, pp. 162–173, 2008.

[2] R. Lima, T. Ishikawa, Y. Imai, M. Takeda, S. Wada, and T. Yamaguchi, "Measurement of individual red blood cell motions under high hematocrit conditions using a confocal micro-PTV system," *Annals of biomed. eng.*, vol. 37, no. 8, pp. 1546–1559, 2009.

[3] W.S. Kamoun, S.S. Chae, D.A. Lacorre, J.A. Tyrrell, M. Mitre, M.A. Gillissen, D. Fukumura, R.K. Jain, and L.L. Munn, "Simultaneous measurement of RBC velocity, flux, hematocrit and shear rate in vascular networks," *Nature Methods*, vol. 7, no. 8, pp. 655–660, 2010.

[4] J.M. Higgins, D.T. Eddington, S. Bhatia, and L. Mahadevan, "Statistical dynamics of flowing red blood cells by morphological image processing," *PLoS Comp. Biology*, vol. 5, no. 2, pp. e1000288, 2009.

[5] K. Palaniappan, F. Bunyak, S.K. Nath, and J. Goffeney, "Parallel processing strategies for cell motility and shape analysis," in *High-Throughput Image Reconstruction and Analysis*, A.R. Rao and G.A. Cecchi, Eds., chapter 3, pp. 39–87. Artech House Publishers, Jan. 2009.

[6] B. Parvin, Q. Yang, J. Han, H. Chang, B. Rydberg, and M.H. Barcellos-Hoff, "Iterative voting for inference of structural saliency and characterization of subcellular events," *IEEE Trans. Image Process.*, vol. 16, no. 3, pp. 615–623, March 2007.

[7] O. Schmitt and M. Hasse, "Morphological multiscale decomposition of connected regions with emphasis on cell clusters," *CVIU*, vol. 113, no. 2, pp. 188 – 201, 2009.

[8] T. Chan and L. Vese, "Active contours without edges," IEEE Trans. Image Process., vol. 10, no. 2, pp. 266–277, Feb. 2001.

[9] V. Caselles, R. Kimmel, and G. Sapiro, "Geodesic active contours," *Int.J. Comput. Vis.*, vol. 22, no. 1, pp. 61–79, 1997.

[10] I. Ersoy, F. Bunyak, K. Palaniappan, M. Sun, and G. Forgacs, "Cell spreading analysis with directed edge profile-guided level set active contours," *Lecture Notes in Computer Science (MICCAI)*, vol. 5241, pp. 376–383, Sep. 2008.

[11] I. Ersoy and K. Palaniappan, "Multi-feature contour evolution for automatic live cell segmentation in time lapse imagery," in *Proc. IEEE Int. Conf. of EMBC*, Aug. 2008, pp. 371–374.

[12] B. Zhang, C. Zimmer, and J.C. Olivio-Marin, "Tracking fluorescent cells with coupled geometric active contours," in *Proc. IEEE Int. Symp. Biomed. Imaging*, April 2004, vol. 1, pp. 476–479.

[13] R. Bise, Z. Yin, and T. Kanade, "Reliable cell tracking by global data association," in *Biomedical Imaging: From Nano to Macro, 2011 IEEE Int. Sym. on*, 2011, pp. 1004 –1010.

[14] E. Meijering, O. Dzyubachyk, I. Smal, and W.A. van Cappellen, "Tracking in cell and developmental biology," in *Seminars in Cell & Dev. Bio.* Elsevier, 2009, pp. 894–902.

[15] D. Padfield, J. Rittscher, and B. Roysam, "Coupled Minimum-Cost Flow Cell Tracking for High-Throughput Quantitative Analysis," *Medical Image Analysis*, 2010.